Experimental Study of Spectral Properties of a Frenkel-Kontorova System

M. Lucci, D. Badoni, V. Merlo, I. Ottaviani, G. Salina, and M. Cirillo*
Dipartimento di Fisica and MINAS Lab, Università di Roma Tor Vergata, 00133 Roma, Italy and INFN sezione "Tor Vergata", via della Ricerca Scientifica, 00133 Roma, Italy

A. V. Ustinov
Physikalisches Institut, Karlsruhe Institute of Technology, D-76128 Karlsruhe, Germany and National University of Science and Technology MISIS, Leninsky prosp. 4, Moscow 119049, Russia

D. Winkler
Department of Microtechnology and Nanoscience–MC2, Chalmers University of Technology, SE-412 96 Göteborg, Sweden

(Received 6 March 2015; published 3 September 2015)

We report on microwave emission from linear parallel arrays of underdamped Josephson junctions, which are described by the Frenkel-Kontorova (FK) model. Electromagnetic radiation is detected from the arrays when biased on current singularities (steps) appearing at voltages $V_n = \Phi_0(n\bar{c}/L)$, where $\Phi_0 = 2.07 \times 10^{-15}$ Wb is the magnetic flux quantum, and $\bar{c}$, L, and n are, respectively, the speed of light in the transmission line embedding the array, L its physical length, and n an integer. The radiation, detected at fundamental frequency $\bar{c}/2L$ when biased on different singularities, indicates shuttling of bunched 2π kinks (magnetic flux quanta). Resonance of flux-quanta motion with the small-amplitude oscillations induced in the arrays gives rise to fine structures in the radiation spectrum, which are interpreted on the basis of the FK model describing the resonance. The impact of our results on design and performances of new digital circuit families is discussed.

DOI: 10.1103/PhysRevLett.115.107002 PACS numbers: 74.50.+r, 85.25.-j, 85.35.Ds

The physics of single flux quanta, or fluxons, (corresponding to 2π kinks of the superconducting phase difference φ) in spatially extended Josephson junctions structures has attracted the attention of the scientific community since the early stages of the research on weak superconductivity [1,2]. Fluxon dynamics served as a relevant experimental test bench for soliton perturbation theory and nonlinear physics [3]. The features of topological kinks in the discrete, nonintegrable, Frenkel-Kontorova model [4,5], implemented by a chain of point-like Josephson junctions connected by inductors to form a one-dimensional (1D) array, has also attracted attention due to the interest for the dynamics of solitons in condensed matter physics [6]. On the practical side, the storage and manipulation of flux quanta in Josephson transmission lines (JTLs) [7] is the physical phenomenon underlying the principles of a successful logic family operating at unprecedented clock frequencies [8].

Recently, new low-dissipative logic families, still relying on Josephson flux quanta as carriers of bits of information [9–11], have been proposed. One of the new logic families [9] relies on moving flux quanta along 1D underdamped arrays in which the Josephson junctions are strongly coupled by inductors along the flux-quanta propagation direction. Here we show evidence that, for this type of array in the strong coupling regime, stable single and multiple flux-quanta propagation exists over broad bias current ranges. Our experiments also confirm predictions of the theoretical modeling of the complex dynamics of 2π kinks in the Frenkel-Kontorova model [9,12–17].

Figure 1(a) displays a photo of a portion of the real device showing the open-ended [13] parallel array of small junctions. The electrodes forming the array of junctions are part of the central conductor of a coplanar waveguide allowing radiation detection. The junctions were window-like fabricated using the standard Nb-AlO_x-Nb trilayer technology [18,19] and had a current density of 110 A/cm^2. The measurements herein presented are part of an investigation performed on arrays which were made of 50, 30, and 25 junctions in parallel; all the measurements were performed at 4.2 K. In Fig. 1(b) we show a detail of the current-voltage (IV) characteristic of a sample corresponding to the geometrical characteristics shown in Fig. 1(a). In this current-voltage (IV) characteristic we see, from left to right, the Josephson current and four zero-field singularities (ZFS) or zero-field steps, which are evidence of flux-quanta motion when the external magnetic field is zero or close to it. These singularities look strikingly similar to the analogous continuous long junctions' case [2], but we shall later evidence significant differences in their radiation spectrum.

In Fig. 2(a), we show a plot of the dc-bias current vs frequency of the emitted radiation, or current-frequency characteristics, for three ZFS of a parallel array of 50 junctions. The radiation emitted by the array was amplified

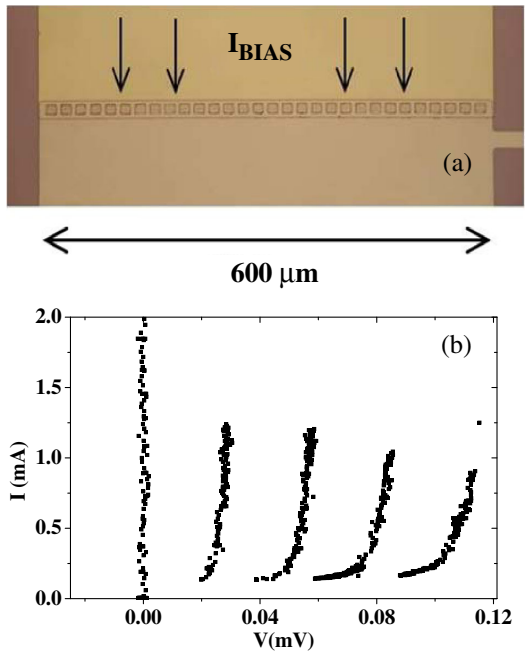

FIG. 1 (color online). (a) Photograph showing a parallel array of junctions; the thin film niobium structure generating the array is part of the central conductor of a coplanar waveguide. The bias current is fed through inductors isolating the junctions from spurious ac components; (b) detail of the current-voltage characteristic of one array like that shown in (a) containing 30 junctions in parallel and 600 μm long. The figure shows the zero-voltage Josephson current and four zero-field singularities representing evidence of fluxon shuttling oscillations in the discrete system.

by a large gain, room-temperature, low noise amplifier (AVANTEK AWT-1816, 43 dB gain and noise figure less than 2.8 dB in the 6–18 GHz range) and then visualized on a spectrum analyzer (Tektronix 2782). The junctions of the array in the case of Fig. 2(a) had physical dimensions (9×9) μm^2 and were separated by 2 μm gaps. Considering the highest value of the emission frequency of the first singularity, $\nu = 7.04$ GHz, and the overall length of the array, which is 600 μm, we calculate the product $\bar{c} = 2L\nu$, which gives 0.085×10^8 m/s and thus $(\bar{c}/c_0) = 0.028$ (here $\bar{c}$ and c_0 are, respectively, the speed of light in the JTL and in vacuum). We also recall that $\bar{c} = 1/(LC)^{1/2}$, where L and C are, respectively, inductance and capacitance per unit length of an array-embedding transmission line. The voltage corresponding to the emitted radiation when biased on the first ZFS—see the IV curve on the right side of Fig. 2(a)—was in the interval (27–29) μV, which is twice what one expects from the Josephson ac equation [20]. The bias current-originated Lorentz force moves flux quanta back and forth along free ends' JTLs: at the ends flux quanta inverts their polarity generating periodic 4π–phase advances instead of the usual Josephson effect 2π advances.

In Fig. 2(a), we also show the bias current-radiation characteristics obtained when biasing the same array on the 2nd and 3rd ZFS appearing in the current-voltage characteristics at "asymptotic" voltages of 56 and 85 μV (see IV on the right side, Fig. 2(c)), which would correspond to Josephson frequencies of 27.1 and 41.1 GHz, respectively. However, one can see in Fig. 2(a) that the fundamental frequency of emission from all three ZFS lies in the same frequency range, namely, between 6.5 and 7.1 GHz. The fact that the radiation is detected in the same frequency range indicates that the phenomenon of fluxon bunching [21] can also be invoked to explain the dynamics of discrete arrays, as found in numerical simulations [13–15]: the motion of two or more flux quanta "glued" together gives rise roughly to the same shuttling oscillation frequency as a single one, although with a ZFS at higher "harmonic" voltage.

From the diffraction patterns of single junctions and two and three junction interferometers we determined the average magnetic penetration depth of the samples [12,13], which was 170 nm and an average Josephson penetration depth $\lambda_{\rm jeff} = 65$ μm, which gives a normalized length of the array $L/\lambda_{\rm jeff} = 9.2$. For reaching the bias points on all the steps of Fig. 2 we observed in most of the cases switching from the lowest part of the Josephson current as shown by the horizontal arrows in the IVs: these indicate that static flux quanta trapped in the JTL start moving at a threshold current and generate a voltage. Thus, the Lorentz force needs a threshold current to overcome the potential barrier pinning flux quanta in their locations [5,12,13,17]. From the current-voltage characteristics of the test junction we also estimated the McCumber parameter [2] $\beta_c = [(2\pi I_c R_{\rm qp}^2 C_{SJ})/\Phi_0] = 30\,780$ and the zero-bias plasma frequency [2] $\nu_{j0} = (1/2\pi)\sqrt{(2\pi I_c/\Phi_0 C)} = 38$ GHz; as a resistance in the definition of β_c we have taken the subgap (or quasiparticle, $R_{\rm qp}$) value and assumed 0.05 F/m^2 for the specific capacitance of the junctions.

The evaluation of the inductance l_0 of a single section of the array (given the speed of light in the transmission line and the specific capacitance of the junctions) enables us to evaluate the discreteness parameter $a = (2\pi l_0 I_c/\Phi_0)^{1/2}$ [5,11,12], where $\Phi_0 = 2.07 \times 10^{-15}$ Wb is the magnetic flux quantum. The parameter a is important for the dynamics of the Frenkel-Kontorova model: for the chip of Fig. 2(a) we calculate that $a = 0.25$, meaning that discretization effects can be relevant for our samples. In Fig. 2(b), we show the measurement of the radiation emitted from a chip having a total length of 500 μm and a larger discreteness parameter $a = 0.35$. This larger value with respect to the previous case is determined by the higher values of the critical current of each junction forming the array [68 μA for the array of Fig. 2(b)] and larger inductance of a single unit of the array (0.58 pH). In Fig. 2(b), we show the radiation detected when biased on the first and on the second ZFS. The radiation is observed at subharmonic Josephson frequencies, when biased on the current singularities,

which appeared at asymptotic voltages of 36 and 72 μV (the IV curve is shown on the right side, Fig. 2d). We note, comparing Figs. 2(a) and 2(b), that the frequency of the emitted radiation is consistent with the ratio between the physical lengths of the arrays which is 1.2, as it should be according to the fact that the emission frequency $\bar{c}/2L$ is mainly determined by the physical length and not by the number of junctions. The slight differences in capacitance and inductance per unit length enter in a square root and give rise only to a few percent difference.

Some features visible in Fig. 2(b), namely, discontinuities and branching of the steps, are also systematically observed on another sample, see Fig. 3, having the same type of planar geometry, in terms of junction area and spacing between junctions. The two samples also had the same inductance per section and discreteness parameter $a = 0.35$ but the sample of Fig. 3 was formed by 30 junctions in parallel for a total physical length of 600 μm: the IV curve of this sample showing the ZFS is the one shown in Fig. 1(b). Notice that the highest emission frequency when biased on the first ZFS of Fig. 3 is 6.93 GHz, very close to that of Fig. 2(a), as it is expected since the arrays have the same physical length and only a few percent difference in electromagnetic wave propagation velocity. Measurements of radiation emission from the 1st and 2nd ZFS of this sample are shown in Figs. 3(a) and 3(b): the observed fine structure of the fluxon steps (in the case of periodic boundary conditions [12,16,17]) and ZFS modes (in the case of open boundary conditions [13]) is due to resonant locking of the fluxon oscillations to the frequency of Josephson plasma waves in the fluxon's tail, which propagate with a phase velocity equal to the fluxon velocity. Note that most of the emission from the 2nd ZFS is measured at double frequency, meaning that both two-bunch fluxon oscillations [Fig. 3(a)] and symmetric fluxon-antifluxon oscillations [Fig. 3(b)] can take place [13].

The locking between the flux quanta moving back and forth along the array and the internal oscillations [22] of the inductively coupled small junctions occurs when one period of the flux-quanta shuttling oscillations matches m periods of the internal small-amplitude oscillations of the junctions: the phenomenon is therefore of discrete nature and it generates the discontinuous shape of the ZFS. In Fig. 3(c), we report the comparison between the theoretical result of Eq. (7) in Ref. [12] for the voltage positions of the fine-structure branches, namely,

$$V_m = \frac{S}{m}\sqrt{1+\frac{4}{a^2}\sin^2\left(\frac{\pi m}{N}\right)}, \tag{1}$$

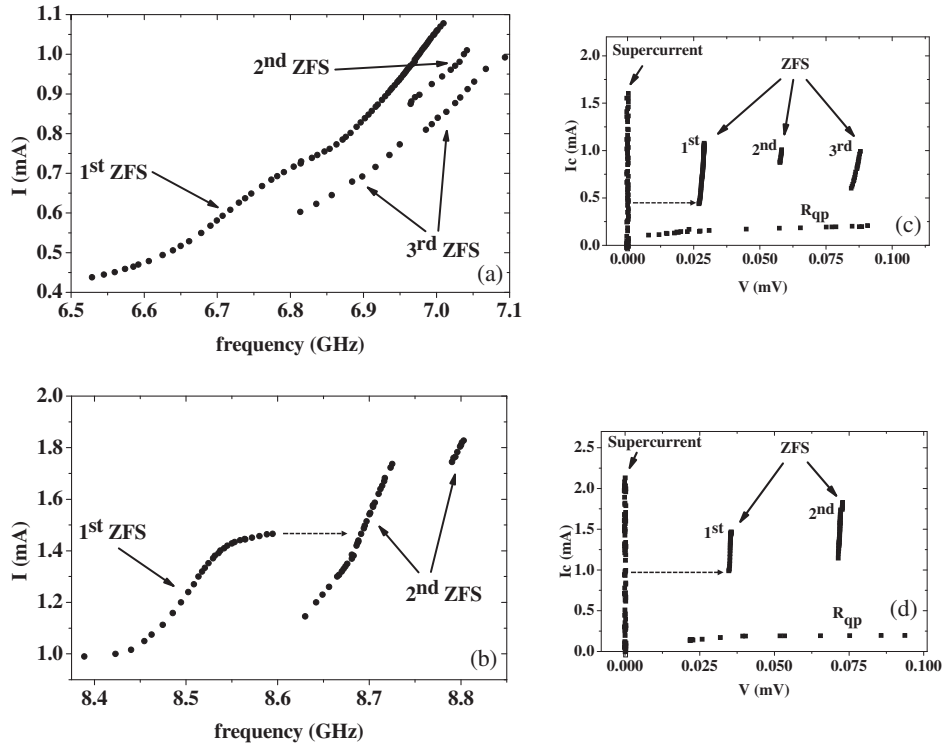

FIG. 2. (a) Subharmonic Josephson radiation detected when biased on the three ZFSs of a 600 μm-long array having discretization parameter $a = 0.25$; (b) detection from 1st and 2nd ZFS of a 500 μm-long, 25 junctions array with discretization parameter $a = 0.35$; both for (a) and (b) radiation is detected at subharmonic Josephson frequencies. (c) and (d) The IV characteristics relative respective to (a) and (b): note that the voltage positions are different by a factor 2 and 3 for the 2nd and 3 rd ZFS, respectively, while the radiation frequency remains in the same range. Second harmonic frequencies of the signals shown in Fig. 2(a) were roughly 10 dB lower in power.

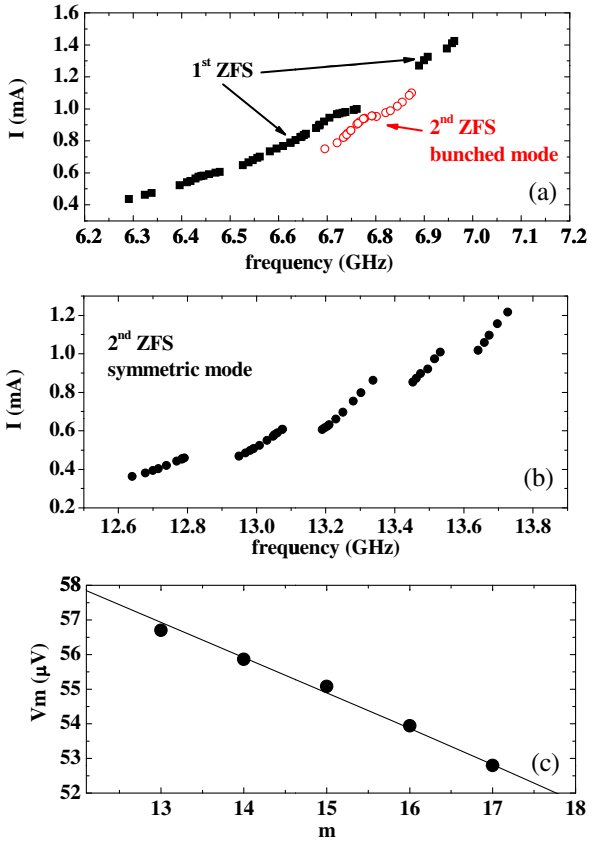

FIG. 3 (color online). (a) Radiation detection from 1st and 2nd ZFS of a 600 μm-long array with discretization parameter $a = 0.35$. The radiation on the 2nd step is relative to a bunched-fluxons mode. (b) The evident, ladderlike structure of the 2nd ZFS accompanied by the radiation from a symmetric fluxon-antifluxon step due to resonances between fluxon motion and low amplitude oscillations of junctions. (c) A fit of the data shown in (b) for the asymptotic position of the branches within the Frenkel-Kontorova phase-locking interaction model.

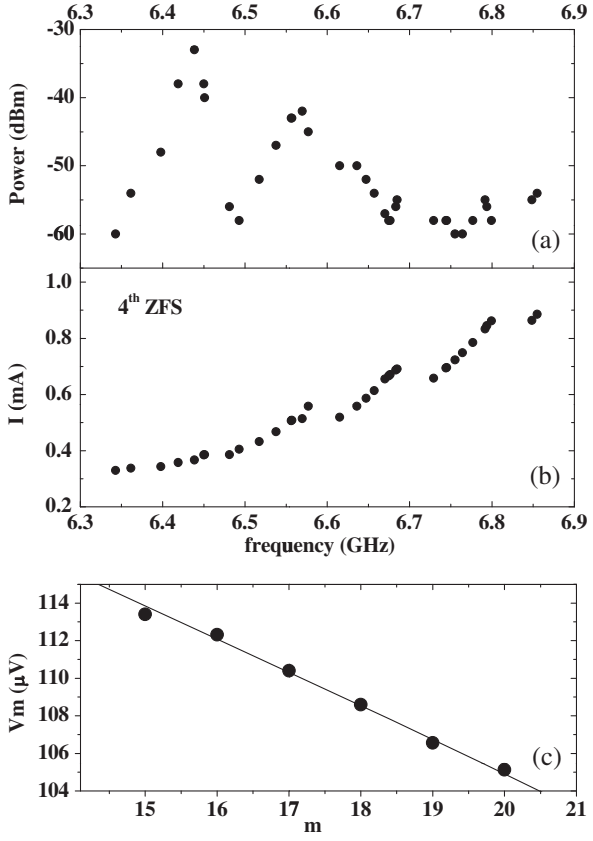

FIG. 4. (a) Emitted power spectrum as a function of frequency when biased on the fourth ZFS of a 600 μm-long array containing 30 junctions [the IV curve is shown in Fig. 1(b)]. (b) Current-frequency characteristic for the sample shown in (a). (c) Fitting of the position of the branches seen in (b) with the fluxon-radiation interaction model. Note in (a) that the power for lower currents is roughly 30 dB above the values for higher frequencies.

and the experimental data of Fig. 3(b) for the 2nd ZFS. In the above equation, $S = \nu_{\mathrm{LC}}\Phi_0$, where $\nu_{\mathrm{LC}} = (1/2\pi)(1/l_0C)^{1/2}$ is the fundamental resonance frequency of the single cell of the array and N the number of junctions of the array. The results are shown in Fig. 3(c) where the voltage V_m is the maximum voltage of the branches visible in Fig. 3(b); note that, when stepping between frequency and voltage on the nth current singularity, the "fluxon" Josephson relations, i.e., $V_n = \Phi_0(n\bar{c}/L)$ were considered. In the fitting, we fixed the parameter a to its experimentally determined value $a = 0.35$.

In Fig. 4, we show data relative to the fourth ZFS of the same sample of Fig. 3. Figure 4(a) presents a plot of the emitted radiation power as a function of its frequency while in Fig. 4(b) we display the characteristic ladderlike structure of the step. The values of the power in (a) correspond to the spectrum analyzer readout and therefore the 43 dB amplification must be subtracted for obtaining the real emitted power. We can see in Fig. 4(a) that the emitted radiation power has a sort of oscillating behaviour and that the maxima are reached close to the top switching points of the lowest branches: here we measure increases up to 30 dB, roughly a factor 10^3 in power. The observed increases of the power were not recorded in previous measurements of continuous junctions meaning that the phenomenon that we observe is unambiguously due to the discreteness of the system. Considering the available dc power in terms of the current-voltage product, from the current vs frequency characteristics of Fig. 4(b) one would expect an increase of a factor 3 of the power between the lowest and the highest values of current and frequency. A "reverse" (higher ac for lower dc power) factor 1000 difference between the bias points on the same current singularity, to our knowledge, has never been observed.

In Fig. 4(c), we show the fit of our data to Eq. (1). As before, the voltage V_m is the maximum voltage of the branches visible in Fig. 4(b). It is worth noting that the value of S in Eq. (1) returned by the fitting procedures of Figs. 3(c) and 4(c) was within 5% of the expected value (calculated from array or junctions geometry and

parameters). The third ZFS displayed features analogous to those of Fig. 4. Our conclusion is that the physical origin of the discontinuous nature of the ZFS is indeed due to the interaction of fluxon motion and low-amplitude oscillations localized along the units of the array. This interaction produces the significant differences between a discrete JTL and its continuum "approximation," namely, the long Josephson junction [1,2]: a continuum approximation for a JTL means, by definition, that wave processes and interactions must vary significantly only over distances encompassing several units and therefore effects generated by oscillations in a single unit are not expected.

In conclusion, microwave spectroscopy has enabled us to characterize the internal dynamics of a Frenkel-Kontorova system and to explain the results in terms of kinks dynamics. A remarkable increase of roughly 3 orders of magnitude of the emitted radiation power observed within the current span of a single resonance indicates that phase coherence in our system could embody other intriguing features. The stability of the bunched oscillations over wide current intervals that we have recorded is an encouraging result for a specific logic family relying on dynamics of groups of kinks for shift register and other functions [9]. However, our results also show that in the underdamped regime the effects of resonances are significant and therefore particular attention should be devoted in the design to prevent circuit configurations which could generate indirect sources of dissipation and/or energy wells in JTLs. In particular, for the RQL [11] logic families, relying on high frequency bias distribution for the logic operations, the identification of any mechanism exciting unwanted resonances or spurious oscillations could be relevant.

This work was partially supported by INFN (Italy) through the DIGITHEL project. A. V. U. acknowledges support by the Ministry for Education and Science of the Russian Federation under Contract No. 11.G34.31.0062 and in the framework of Increased Competitiveness Program of the National University of Science and Technology MISIS under Contract No. K2-2014-025.

*Also at *CNR-SPIN* Institute, via Giovanni Paolo II, 84084 Fisciano, Italy.

[1] A. C. Scott, Am. J. Phys. **37**, 52 (1969); J. R. Waldram, A. B. Pippard, and J. Clarke, Phil. Trans. R. Soc. A **268** (265 (1970); T. A. Fulton, R. C. Dynes, and P. W. Anderson, Proc. IEEE **61**, 28 (1973).

[2] A. Barone and G. Paternò, *Physics and Applications of the Josephson Effect* (Wiley, New York 1982), Chap. 10.

[3] D. W. McLaughlin and A. C. Scott, Phys. Rev. A **18**, 1652 (1978).

[4] T. A. Kontorova and Ya. I. Frenkel, Zh. Eksp. Teor. Fiz. **8**, 89 (1938); **8**, 1340 (1938).

[5] M. Peyrard and M. Kruskal, Physica (Amsterdam) **14D**, 88 (1984); J. F. Currie, S. E. Trullinger, A. R. Bishop, and J. A. Krumhansl, Phys. Rev. B **15**, 5567 (1977).

[6] O. M. Braun and Y. S. Kivshar, Phys. Rep. **306**, 1 (1998); D. L. Campbell, S. Flach, and Y. S. Kivshar, Phys. Today 57, 43 (**2004**).

[7] M. Cirillo, J. Appl. Phys. **58**, 3217 (1985).

[8] K. K. Likharev and V. K. Semenov, IEEE Trans. Appl. Supercond. **1**, 3 (1991).

[9] V. K. Semenov, G. V. Danilov, and D. V. Averin, IEEE Trans. Appl. Supercond. **13**, 938 (2003); J. Ren and V. K. Semenov, IEEE Trans. Appl. Supercond. **21**, 780 (2011).

[10] O. A. Mukhanov, IEEE Trans. Appl. Supercond. **21**, 760 (2011); M. H. Volkmann, A. Sahu, C. J. Fourie, and O. A. Mukhanov, Supercond. Sci. Technol. **26**, 015002 (2013).

[11] Q. P. Herr, A. Y. Herr, O. T. Oberg, and A. G. Ioannidis, J. Appl. Phys. **109**, 103903 (2011); O. T. Oberg, Q. P. Herr, A. G. Ioannidis, and A. Herr, IEEE Trans. Appl. Supercond. **21**, 571 (2011).

[12] A. V. Ustinov, M. Cirillo, and B. A. Malomed, Phys. Rev. B **47**, 8357 (1993).

[13] M. Cirillo, B. H. Larsen, A. V. Ustinov, V. Merlo, V. A. Oboznov, and R. Leoni, Phys. Lett. A **183**, 383 (1993); A. V. Ustinov, M. Cirillo, B. H. Larsen, V. A. Oboznov, P. Carelli, and G. Rotoli, Phys. Rev. B **51**, 3081 (1995).

[14] A. V. Ustinov, B. A. Malomed,and S. Sakai, Phys. Rev. B **57**, 11691 (1998).

[15] J. Pfeiffer, M. Schuster, A. A. Abdumalikov, Jr., and A. V. Ustinov, Phys. Rev. Lett. **96**, 034103 (2006).

[16] H. S. J. van der Zant, T. P. Orlando, S. Watanabe, and S. H. Strogatz, Phys. Rev. Lett. **74**, 174 (1995).

[17] J. Pfeiffer, A. A. Abdumalikov, Jr., M. Schuster, and A. V. Ustinov, Phys. Rev. B **77**, 024511 (2008).

[18] M. Gurwitch, W. A. Washington, and H. A. Huggins, Appl. Phys. Lett. **42**, 472 (1983).

[19] J. G. Caputo and L. Loukitch, Physica (Amsterdam) **425C**, 69 (2005); Eur. Phys. J. Spec. Top. **147**, 95 (2007); R. Monaco, G. Costabile, and N. Martucciello, J. Appl. Phys. **77**, 2073 (1995).

[20] T. A. Fulton and R. C. Dynes, Solid State Commun. **12**, 57 (1973).

[21] B. Dueholm, O. A. Levring, J. Mygind, N. F. Pedersen, O. H. Soerensen, and M. Cirillo, Phys. Rev. Lett. **46**, 1299 (1981).

[22] H. H. Zappe and B. S. Landman, J. Appl. Phys. **49**, 344 (1978); G. Paternò, A. M. Cucolo, and G. Modestino, J. Appl. Phys. **57**, 1680 (1985).